

Yttrium Silicate Coatings on Chemical Vapor Deposition-SiC-Precoated C/C–SiC: Thermodynamic Assessment and High-Temperature Investigation

Hans J. Seifert^{*,†}

Department of Materials Science and Engineering, University of Florida, Gainesville, FL 32611-6400

Sigrid Wagner, Olga Fabrichnaya, Hans L. Lukas, and Fritz Aldinger^{*}

Max-Planck-Institut für Metallforschung and Institut für Nichtmetallische Anorganische Materialien, Universität Stuttgart, Pulvermetallurgisches Laboratorium, 70569 Stuttgart, Germany

Thomas Ullmann

German Aerospace Center, Institute of Structures and Design, 70569 Stuttgart, Germany

Martin Schmücker and Hartmut Schneider^{*}

German Aerospace Center, Institute for Materials Research, 51147 Cologne, Germany

Yttrium silicates are promising materials for improved oxidation and erosion protection for carbon fiber-reinforced composites. A two-layer coating system of low-pressure plasma-sprayed yttrium silicate on chemical vapor deposition-SiC-precoated C/C–SiC was tested under atmospheric re-entry conditions simulated within a plasma wind tunnel test facility. The thermal expansion behavior of Y_2SiO_5 and $Y_2Si_2O_7$ was investigated. The chemical compatibility with and without increasing oxygen partial pressure at the interface of the two-layer system was calculated by the CALPHAD method. The calculations were compared with experimental results. Furthermore, a thermodynamic explanation is presented to understand and predict the observed coating failure mechanism, identified as blister formation.

I. Introduction

BECAUSE of their mechanical strength at high temperatures and their thermal shock resistance in combination with low specific mass, carbon fiber-reinforced composites like C/C–SiC are promising materials for high-temperature structural applications in gas turbines or heat shields of aerospace re-entry vehicles. In oxidative environments, protective coatings are required because of the degradation of carbon at temperatures above 673 K. The coating has to be oxidation resistant and has to prevent oxygen diffusion inwards as well as carbon diffusion outwards in order to avoid oxidation or carbothermic reduction. During the atmospheric re-entry maneuver of a space vehicle, the low-pressure environment and the surrounding high-velocity plasma flow have to be considered. Therefore, the coating material must possess low volatility to prevent excessive surface erosion. To provide adequate adhesion between the coating and the substrate, and mechanical stability of the system, the coefficient of thermal expansion (CTE) of both have to be as similar

as possible. It is generally accepted that to fulfill all these fundamental requirements in a high-temperature oxidizing environment, a multilayer coating is needed rather than a single-layer coating.^{1–3}

Silicon-based ceramic coatings, like SiC or Si_3N_4 , are attractive materials for oxidation protection at elevated temperatures for extended time periods because of their thermophysical properties, as well as the formation of a thin amorphous SiO_2 scale with simultaneous low oxidation rate.⁴ The occurrence of microcracks within the coating, which is a result of thermo-mechanically induced stress, is problematic and to avoid this effect it is proposed to introduce single layers or inlays of a glass-forming phase to provide self-healing capabilities.^{2,3} Many multilayer systems have been developed, containing one or more glass sealant layers covered with inner and outer ceramic layers.³

In view of applicability as a coating material, Ogura *et al.*⁵ investigated the thermal properties of monosilicates from lanthanides (Ln_2SiO_5) and yttrium (Y_2SiO_5). It has been demonstrated that yttrium monosilicate (Y_2SiO_5 , MS) has the potential to be used as an erosion-resistant layer. Therefore, a two-layer system for C/C composites has been proposed, consisting of an inner SiC bonding layer and an outer oxidation/erosion protection layer of yttrium monosilicate. The aim is to design a coating system that is inherently crack resistant without using expensive sealing layers,⁶ as for example B_4C applied by chemical vapor deposition (CVD). Because of the low Young's modulus of Y_2SiO_5 and the high compatibility of the CTEs between SiC and Y_2SiO_5 , the mechanical-induced stress at the Y_2SiO_5 –SiC interface is decreasing significantly.⁵ On the other hand, the formation of gaseous oxidation products between the oxide and the carbide layers becomes serious with increasing temperature.^{3,7–9}

To produce dense yttrium silicate coatings, it has been found that the presence of yttrium disilicate ($Y_2Si_2O_7$, DS) in the outer yttrium silicate layer is useful.^{9,10} In this work, a low-pressure plasma spray (LPPS) technique is used to produce yttrium silicate coatings on CVD-SiC-precoated C/C–SiC specimens (58.4% carbon fiber content), manufactured via liquid silicon infiltration.¹¹ The oxidation and erosion protection efficiency under simulated atmospheric re-entry conditions are compared with specimens protected only with a CVD-SiC layer and with industrial-manufactured multilayer coatings, based on SiC. During the tests in a plasma wind tunnel facility, at temperatures above 1923 K,¹⁰ a sudden coating failure has been

D. Butt—contributing editor

Manuscript No. 187370. Received October 26, 2001; approved September 3, 2004. Supported by the German Research Foundation (SFB259, High Temperature Problems of Reusable Space Transportation Systems).

^{*}Member, American Ceramic Society.

[†]Author to whom correspondence should be addressed. e-mail: hseif@mse.ufl.edu

observed, identified as the formation of blisters. Spallation of a yttrium silicate coating was also observed by Webster *et al.*⁹ during continuous isothermal mass change measurements in air at 1873 K. Discussed as a mismatch of CTE,¹⁰ the aim of this work is to give an explanation for the failure mechanism. The thermal expansion behavior of Y_2SiO_5 and $Y_2Si_2O_7$ is investigated and compared with published results. Apparently, the mismatch in CTE cannot be the only reason for the observed coating failure. Thermodynamic calculations are carried out to understand possible interface reactions between yttrium silicate and SiC with increasing oxygen partial pressure.

II. Thermodynamic Database

The CALPHAD (CALculation of PHase Diagrams¹²) method is used to determine phase equilibria and phase reactions in multicomponent systems. A consistent set of thermodynamic data for the Y-Si-C-O was developed and the calculations were carried out using ThermoCalc software.¹³ The unary data for the pure elements and the description for the gaseous species were taken from the SGTE substance database.¹⁴ The thermodynamic description for the binary systems Y-Si, Y-C, Si-C, and Y-O were derived by thermodynamic optimization^{15,16} and the system Si-O was taken from the literature.¹⁷ Based on phase diagram data and measurements of enthalpy of formation and heat capacity for the solid phases,^{18,19} a thermodynamic assessment of the system Y_2O_3 -SiO₂ was performed.²⁰ For the description of the liquid phase, the two-sublattice liquid model was used. The descriptions were combined in one single database to calculate the phase equilibria in the quaternary Y-Si-C-O system.

III. The Pseudobinary System Y_2O_3 -SiO₂

In the system Y_2O_3 -SiO₂, two yttrium silicate compounds are known: Y_2SiO_5 and $Y_2Si_2O_7$.^{21,22} The monosilicate (Y_2SiO_5) occurs in two different modifications (designated as X₁ and X₂) and the disilicate ($Y_2Si_2O_7$) occurs in four different modifications (referred to as α , β , γ , and δ ; in order of increasing temperature). The phase transitions are of reconstructive character and the transition temperatures are given by Felsche.²¹ Those between the $Y_2Si_2O_7$ modifications are very sluggish. The modification change of Y_2SiO_5 is martensitic;²³ both Y_2SiO_5 structures are of monoclinic symmetry and crystallize within point group 2/c. The difference lies in the unit cell: While the high-temperature modification (X₂) is base centered, X₁ crystallizes in a primitive cell.²² The calculated pseudobinary system is shown in Fig. 1.²⁰ The calculations do not take into account the polymorphic transformation of Y_2SiO_5 . According to the calculations, Y_2SiO_5 melts congruently at 2232 K, and δ - $Y_2Si_2O_7$ melts incongruently at 2060 K.

IV. Experimental Procedure

Y_2SiO_5 and $Y_2Si_2O_7$ were prepared by the mixed-oxide technique. Starting materials were powders of high purity of Y_2O_3 (Alfa, 99.99%, <1 μ m, Alfa Aesar, Karlsruhe, Germany) and SiO₂ (Chempur, 99.99%, <45 μ m, Karlsruhe, Germany). Prior to use, the oxides were dried at 1273 and 1073 K, respectively, and subsequently stored in a desiccator. Appropriate amounts of oxides were mixed for 24 h in a 3-D powder mixer. The powder mixtures were isostatically cold pressed at 800 kPa and annealed for 120 h at 1873 K in air, with intermediate milling. By this treatment, pure yttrium silicates were obtained as confirmed by XRD and energy-dispersive X-ray spectroscopy (EDS) measurements.

The CTEs of the pure yttrium silicates (MS and DS) were measured on cylindrical samples (0.5 cm \times 0.3 cm, 98.7% theoretical density) with a differential dilatometer (Model 802, Bähr, Hüllhorst, Germany) and heating up to 1673 K in air with a gradient of 5 K/min.

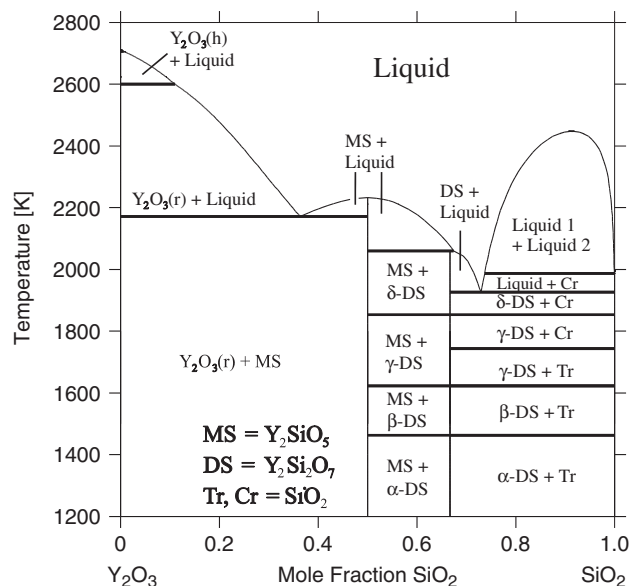


Fig. 1. The calculated Y_2O_3 -SiO₂ system.²⁰

To examine possible reactions between SiC and Y_2SiO_5 , the Y_2SiO_5 was milled and mixed with β -SiC (Cerac Inc., 99.9%, <1 μ m, Milwaukee, WI). Bulk samples were prepared as described above and annealed for 8 and 128 h, respectively, at 1923 K in air. Additionally, thermogravimetric analysis (TGA) was carried out on these samples in air up to 1923 K (Bähr STA501) using an Al₂O₃ crucible, which was covered inside with platinum foil. The phase compositions were analyzed by XRD (Siemens Diffractometer D5000/Kristalloflex, CuK α ₁ radiation, Bruker AXS, Karlsruhe, Germany). The evaluation was performed by using Bruker AXS DIFFRAC AT software, comparing with the Powder Diffraction File data of the International Centre for Diffraction Data.

Yttrium silicate coatings were deposited on CVD-SiC-precoated C/C-SiC specimens by an LPPS technique.¹⁰ This process is based on the generation of a plasma jet consisting of an argon gas flow with admixtures of hydrogen and helium. The gas flow is ionized while passing a high current arc discharge within the plasma torch. The plasma jet leaves the torch by passing a Laval-nozzle with a plasma jet velocity of up to 3000 m/s. When powder is injected into the plasma jet, the particles will be accelerated (>800 m/s) and molten before being projected onto the substrate.²⁴ Two yttrium silicate powders of different composition were sprayed, as given in Table I. The coating thickness of the yttrium silicate layers varied between 100 and 200 μ m.²⁵

The C/C-SiC specimens with coatings obtained by spray powder 1 (Table I) were tested within a plasma wind tunnel test facility²⁶ to assess the oxidation and erosion resistance under simulated atmospheric re-entry conditions. The vacuum chamber of the test facility is a 5 m long steel tank with a diameter of 2 m, divided into three cylindrical segments, which all have a double-wall cooling segment.¹⁰ The sample geometry is shown in Fig. 2. During these tests, the sample was attached to a

Table I. Chemical Composition and Particle Size Fraction of the Plasma-Sprayed Powders

	Spray powder 1	Spray powder 2
Composition Y_2O_3 :SiO ₂	50:50 wt% 21:79 at. %	75.5:24.5 wt% 45:55 at. %
Particle size distribution (μ m)	8–25	5–30
Median size (μ m)	19.9	16.7
Phase content	$Y_2Si_2O_7$ +SiO ₂	Y_2SiO_5 + $Y_2Si_2O_7$

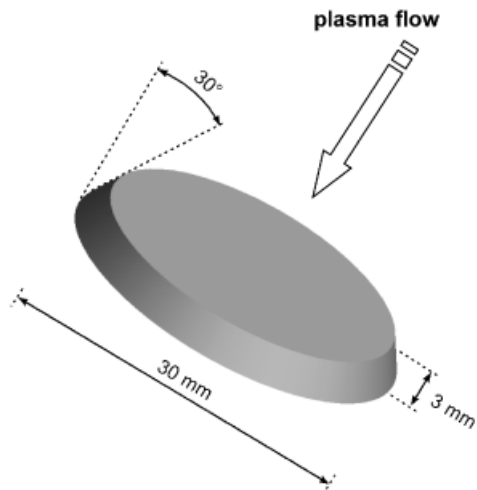


Fig. 2. Sample geometry for the plasma wind tunnel tests.

water-cooled support system, which is mounted on a movable platform of the positioning system. The sample itself was mounted inside a sample support cap, which is made of sintered SiC and faced toward the plasma source. As indicated by the arrow in Fig. 2 (plasma flow direction), a circular-shaped area of the sample's surface (diameter: 26.5 mm) was exposed to a plasma flow of approximately 800 m/s.

The chosen test parameters were the same as those from previous successful test campaigns of other projects,^{10,27} with CVD-SiC-coated C/C-SiC and multilayer-coated C/SiC samples supplied by MAN Technology (Munich, Germany) and by Astrium (Friedrichshafen, Germany), respectively. With mass flow rates of 1.6 g/s N₂ and 0.4 g/s O₂, respectively, the stagnation pressure was approximately 4.1 mbar. For the possibility of direct comparison of specimens with different coating systems, the first tests with the two-layer LPPS/CVD coating system were performed at 1623 K for 23 min at maximum temperature. The following tests at 1773, 1873, and 1923 K, respectively, were performed by increasing the current of the plasma generator. The specific mass loss was determined by the sample's change in mass versus testing time.

V. Results and Discussion

(1) Mass Loss During Plasma Wind Tunnel Tests

After 23 min at 1623 K in the plasma wind tunnel, the visual appearance of the test specimens with yttrium silicate coatings obtained from powder 1 changed. The typical gray color of the coating turned into white—just as the color of the original spray powder—and the coating surface appeared smoother because of

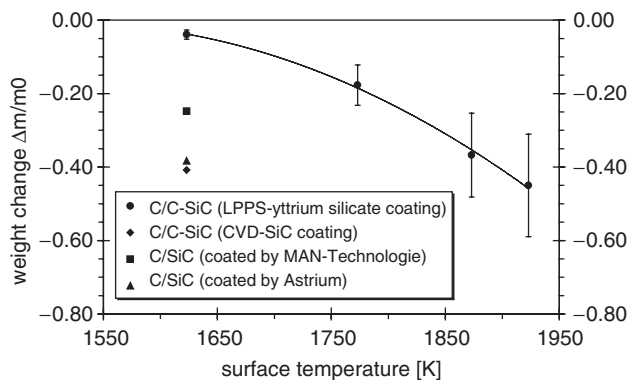


Fig. 3. Relative mass loss with coated C/SiC and C/C-SiC specimens after plasma wind tunnel testing (23 min at maximum temperature with N₂: O₂ = 80: 20 wt% and $p = 4.1$ mbar).

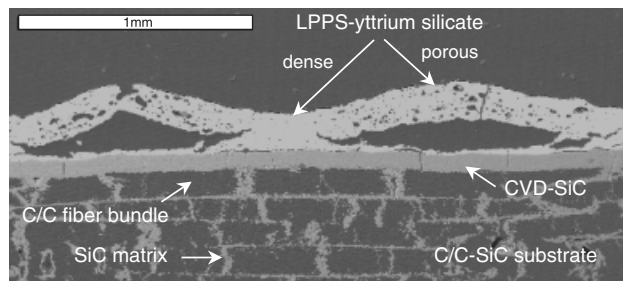


Fig. 4. Blister formation as observed at test temperatures above 1923 K.¹⁰

sintering effects. However, investigations by SEM did not show any apparent degradation within the C/C-SiC substrate material. As shown in Fig. 3, at 1623 K, the weight change of C/C-SiC specimens with yttrium silicate protection is less than 10% that of samples with a CVD-SiC coating. Also, the C/SiC material with coating systems from industrial suppliers show a weight loss approximately six times (MAN Technology)²⁷ and 10 times (Astrium)²⁷ higher than that of C/C-SiC material with an LPPS-yttrium silicate coating. Higher weight loss indicates higher erosion and/or active oxidation of the materials.

At temperatures above 1923 K,¹⁰ a sudden coating failure was observed by visual inspection of the samples during the running tests. The failure always started with the formation of some local hot spots on the sample's surface. Overheating effects like this may be set off by additional heat fluxes resulting from catalytic interaction between the coating's surface and high reactive components of the plasma flow, as for example the recombination reaction of atomic oxygen. By the following SEM investigation, these hot-spot areas have been identified as areas of blister formation. As an example, Fig. 4 shows the beginning spallation of yttrium silicate coating that was obtained with spray powder of type 2 (Table I). Besides the cracks with parallel orientation to the Y₂SiO₅/Y₂Si₂O₇-SiC interface, numerous small cavities or bubble-like structures are visible within the loosened silicate layer, which indicates increasing porosity and gaseous reaction products. These areas are in contrast to the almost undisturbed coating in between the blisters (Fig. 4, middle). Here the original low-pressure plasma-sprayed coating with its dense microstructure (porosity ≤ 1%) as obtained with spray powder 2 is still visible.

In view of coating failure mechanisms, the deficiencies of mechanical or chemical compatibility between the coating materials and the substrate are important aspects to discuss.

(2) Mechanical Compatibility

Because of a mismatch in the CTE of phases within a multilayer coating and the substrate, the cooling process after the coating deposition will cause multiple microcracks and thus increasing ingress of oxygen.

In Fig. 5, the results of thermal expansion measurements of both yttrium silicates are shown. For comparison, literature data of SiC are also shown.^{5,28} The mean CTE of Y₂Si₂O₇ is determined to $4.84 \times 10^{-6}/\text{K}$ (300–1673 K) and therefore, it is presumed to be close to that of the SiC substrates ($4.3\text{--}5.4 \times 10^{-6}/\text{K}$ determined in the ranges from 297 to 1144 K and from 811 to 2477 K, respectively). This was also found by Aparicio and Duran²⁸ ($4.6 \times 10^{-6}/\text{K}$ for 300–1273 K). Thus Y₂Si₂O₇ and SiC can be considered as mechanically compatible. Therefore, with increasing amount of Y₂Si₂O₇/Y₂SiO₅ ratio, the plasma-sprayed coating is expected to show higher mechanical compatibility to the SiC sublayer and the C/C-SiC substrate.

Ogura *et al.*⁵ reported that the mean CTE of polycrystalline Y₂SiO₅ is $4.8 \times 10^{-6}/\text{K}$ (300–1623 K), which is also close to that of SiC. According to Ogura's XRD analysis, the bulk samples contained Y₂O₃ as a minor constituent. Aparicio and Duran²⁸ determined for the yttrium monosilicate a higher value of $6.9 \times 10^{-6}/\text{K}$ in the range from 300 to 1273 K, measured on

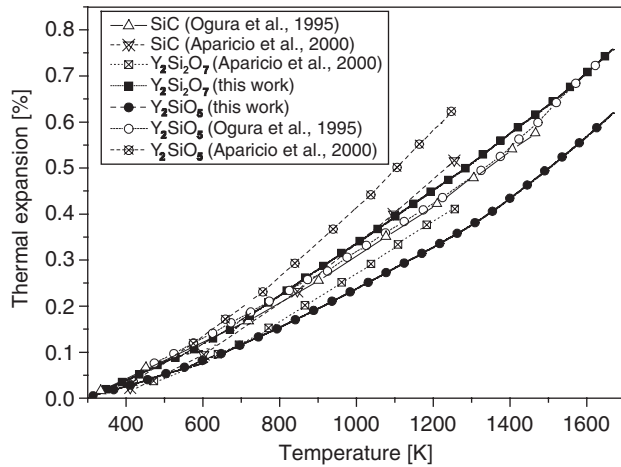
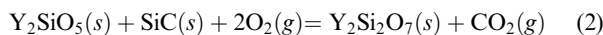
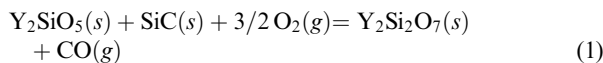


Fig. 5. Thermal expansion of yttrium silicates and SiC.

bulk sample prepared by mixing oxides and heat treating at 1833 K for 3 h. The preparation in this way also leads to a small amount of residual Y_2O_3 , as shown by XRD patterns in Aparicio *et al.*²⁹ The mean CTE of Y_2O_3 is $9.5 \times 10^{-6}/K$,²⁸ which means that the presence of some Y_2O_3 should increase the thermal expansion somewhat. As depicted in Fig. 5, both authors are in disagreement with the data of this work. However, the general shape of the mean thermal expansion curve coincides with Ogura *et al.*⁵ At temperatures above approximately 1273 K, the curve of the MS shows obviously an increasing gradient. This can be explained by the mentioned phase transformation of Y_2SiO_5 . According to Nowok *et al.*,²³ the phase transformation takes place at about 1123 K. This is in good agreement with our result,³⁰ observing a transformation temperature of approximately 1173 K. The mean CTE was determined to $3.05 \times 10^{-6}/K$ for 300–1173 K and $4.09 \times 10^{-6}/K$ in the temperature range between 1173 and 1673 K. Thus the phase transformation of Y_2SiO_5 probably causes microcracks during high-temperature application of coatings containing the monosilicate Y_2SiO_5 .

(3) Chemical Compatibility

According to thermodynamic calculations by Webster *et al.*,⁶ carried out for a dense two-layer coating consisting of pure Y_2SiO_5 and SiC, chemical reactions are not expected between the two compositions at temperatures up to 2023 K. Increasing the oxygen content at the Y_2SiO_5 -SiC interface leads to the formation of $Y_2Si_2O_7$ and gas (CO/CO₂) at 1873 K and a mass gain of approximately 6 mass%. Possible reactions between the silicate and the carbide material in the presence of oxygen are given by Webster *et al.*:⁶



According to our thermodynamic calculations, in the absence of any oxidizing gas, the phases Y_2SiO_5 , $Y_2Si_2O_7$, and SiC are in equilibrium up to the incongruent melting of δ - $Y_2Si_2O_7$ at 2060 K (Fig. 6). Therefore, the chemical compatibility is not influenced by the presence of $Y_2Si_2O_7$. The SEM image of such a coating system is shown in Fig. 7. In the cross-section, the light gray LPPS- $Y_2Si_2O_7/Y_2SiO_5$ layer, as obtained with spray powder of type 1 (Table I), and the dark gray CVD-SiC bonding layer underneath are clearly visible. Besides the silicate phases, the plasma-sprayed coating is interspersed by angular—sometimes even rounded—particles of amorphous silica as confirmed by EDS analysis. Obviously, they are residuals resulting from the spray powder that also contains free silica. Chemical reac-

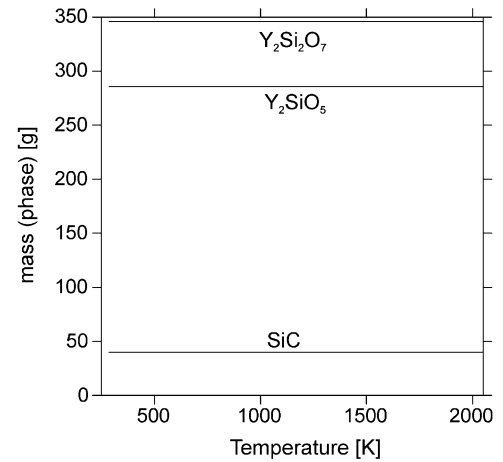
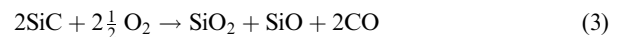


Fig. 6. Chemical compatibility of a ($Y_2SiO_5/Y_2Si_2O_7$) layer on a SiC layer.

tions at the interface of the LPPS- $Y_2Si_2O_7/Y_2SiO_5$ -SiO₂ layer and the CVD-SiC coating have not been observed even after thermal treatment up to 1873 K.

Figure 8(a) shows the calculated phase distribution caused by chemical reactions at the interface of yttrium silicates and SiC at 1923 K with increasing oxygen partial pressure (pO_2). To simulate such conditions, argon (Ar) was formally introduced as an inert gas. This simulation for a closed system is based on the assumption of a silicate composition of 0.33 mole $Y_2Si_2O_7$ and 0.67 mole Y_2SiO_5 to react with 1 mole of SiC. The existence of a small amount of gaseous phase, resulting for example from the ingress through microcracks at ambient pressure of 1 bar, was also taken into account. Because of an accurate determination of the partial pressure of oxygen (pO_2) within the gaseous phase, some predicted chemical reaction mechanisms can be verified. According to Fig. 8(a), Y_2SiO_5 , $Y_2Si_2O_7$, SiC, and gas phase stay in equilibrium as long as the pO_2 does not exceed 3×10^{-16} bar. Above this value, Y_2SiO_5 and SiC react to form $Y_2Si_2O_7$ and gas phase (mainly consisting of CO), as predicted by Webster *et al.*⁶ (Eqs. (1) and (2)). The calculations show that remaining SiC may react with oxygen according to the reaction



As the oxygen partial pressure pO_2 exceeds 5×10^{-15} bar, solid SiO_2 becomes a stable phase. According to the calculations for higher oxygen partial pressures (including conditions in air), $Y_2Si_2O_7$ and SiO_2 remain as the only stable solid phases with a total sample mass gain of 8.6%. It is important to note that the experimentally observed transition from active to passive oxidation of SiC at 1923 K occurs at remarkably higher

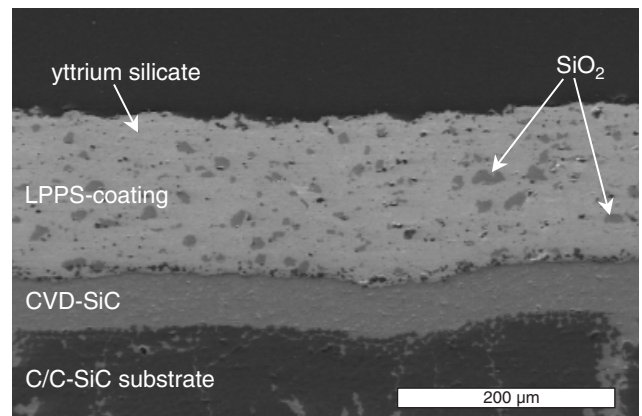
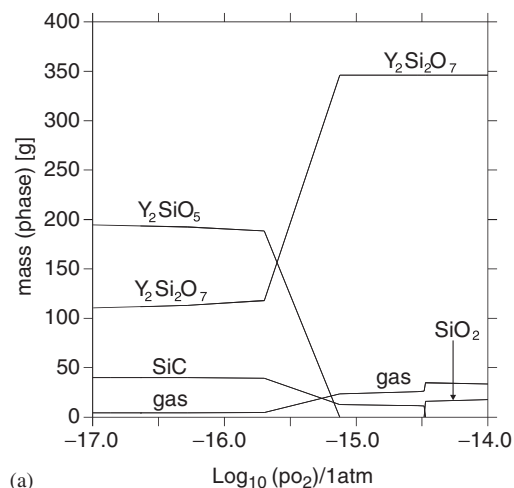
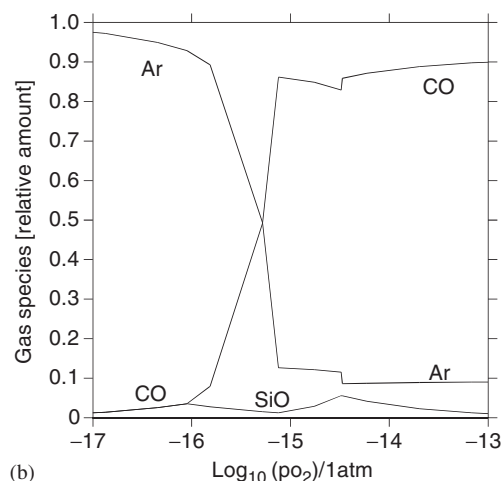


Fig. 7. Cross-section of a two-layer coating system (SEM image).



(a)



(b)

Fig. 8. Thermodynamic simulation of the interface reactions of $Y_2Si_2O_7$ (0.33 mole) and Y_2SiO_5 (0.67 mole) with SiC (1 mole) at 1923 K with increasing oxygen partial pressure. (a) Calculated phase equilibria. (b) Related formation of gas species.

pO_2 ($\sim 10^{-3}$ bar)^{31–33} as compared with the calculated value of 5×10^{-15} bar for the SiO_2 formation. To understand this effect, the mass balance conditions in the treated thermodynamic system have to be taken into account as discussed in detail by Heuer and Lou.³⁴ However, the mechanism of active-passive oxidation is different from the one treated in this work for reactions proceeding at the interface of yttrium silicate and SiC. The coating of 100–200 μm $Y_2SiO_5/Y_2Si_2O_7$ protects the SiC layer until the reaction on the interface creates a gas phase of sufficiently high pressure to delaminate the coating as discussed below.

Figure 8(b) shows the evolution of the relative gas phase composition related to the oxygen partial pressure at 1923 K. The dominating gas species are CO and SiO. At low-oxygen partial pressures, the ratio of both gaseous components is equivalent because both of them are generated from oxidation of SiC only. With higher partial pressures of oxygen, the formation of $Y_2Si_2O_7$ also increases the production of CO significantly while SiO is not involved.

To confirm the results of the simulation, a corresponding powder mixture of 0.67 mole Y_2SiO_5 and 1.0 mole SiC was isostatically cold pressed at 800 kPa and annealed at 1923 K in air for 8 or 128 h, respectively. $Y_2Si_2O_7$ was not added, in order to observe its expected formation. The XRD patterns for this experimental investigation are shown in Fig. 9. After annealing the sample for 8 h, Y_2SiO_5 is still present, but the formation of $Y_2Si_2O_7$ has started and SiO_2 is clearly detectable. After annealing for 128 h, only $Y_2Si_2O_7$ and SiO_2 (cristobalite) could be

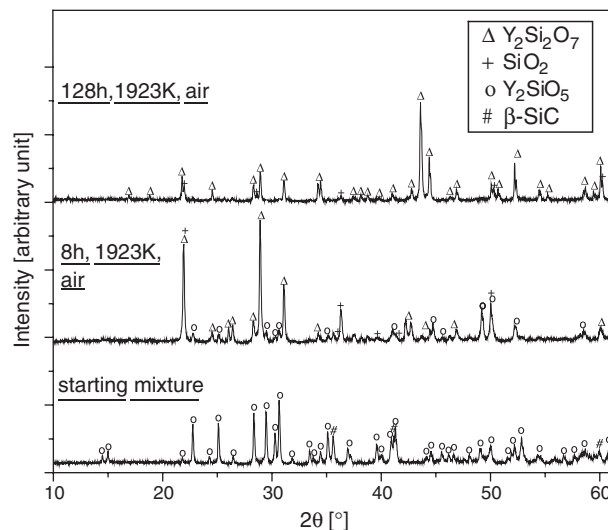


Fig. 9. XRD patterns of the investigated Y_2SiO_5/SiC mixture before and after heat treatment at 1923 K in air.

identified by XRD, in agreement with the calculations. The TGA (Fig. 10) indicates a mass gain of 8.5 mass%, which is in good agreement with the calculated value of 8.6 mass%.

The calculations show that the gas phase consists mainly of CO and SiO species interacting with the solid phases of the system (Fig. 8(b)). Figure 11 shows three calculated isothermal potential phase diagrams (1853, 1903, and 2000 K) illustrating the stabilities of the solid phases as a function of the CO and SiO partial pressures. A triangle-shaped three-phase field can be seen, in which SiC and Y_2SiO_5 are in equilibrium with the gas phase, existing in between four-phase equilibria lines with, e.g. $Y_2Si_2O_7$ or graphite additionally in equilibrium. Since CVD-SiC coatings often contain very small and more or less dispersed inclusions of residual free carbon,³⁵ the intercept point of the lower and upper limiting line of the triangle-shaped phase field is of special interest. At this point, all five phases (gas, SiC, Y_2SiO_5 , $Y_2Si_2O_7$, and graphite) are in equilibrium.

At 1903 K the five-phase equilibria point (gas, SiC, Y_2SiO_5 , $Y_2Si_2O_7$, and graphite) reaches a pCO of 1 bar. At 2000 K, the intersection is outside the chosen axis limit in Fig. 11. For all temperatures, the composition of the gas phase is clearly dominated by pCO (approximately 10 times higher than $pSiO$). Figure 12 illustrates the evolution of the vapor pressure in equilibrium with the four solid phases, graphite, SiC, Y_2SiO_5 , and $Y_2Si_2O_7$, as a function of temperature. As the total pressure of the generated gaseous phase increases drastically with temperature, an equilibrium vapor pressure of approximately 10 bar was calculated for example at 2175 K. These calculations show that

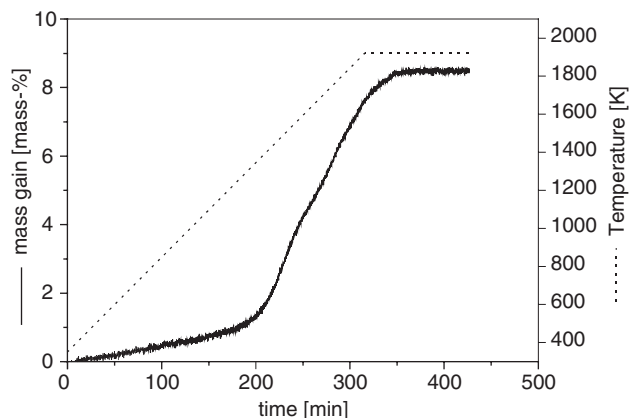


Fig. 10. Thermogravimetric analysis of the Y_2SiO_5/SiC mixture in air between RT and 1923 K.

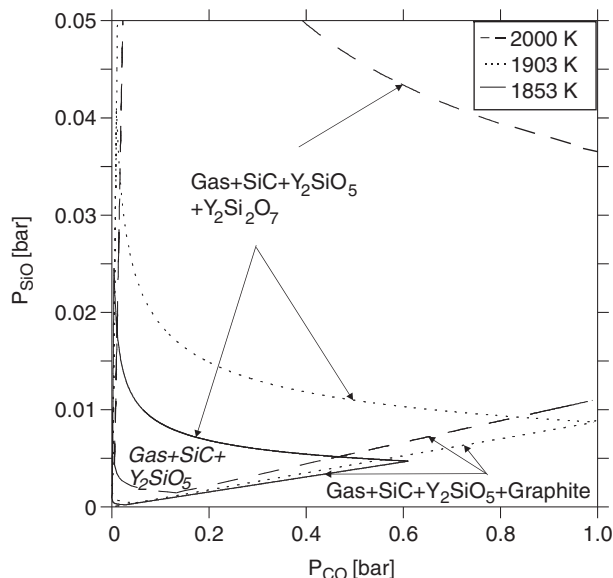


Fig. 11. Potential phase diagrams at 1853, 1903, and 2000 K, respectively.

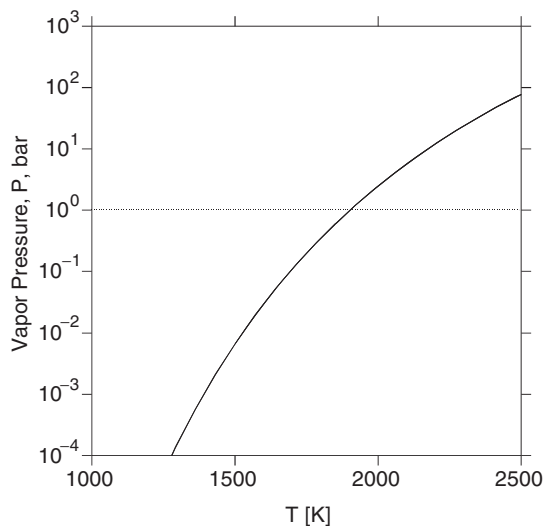


Fig. 12. Vapor pressure in equilibrium with SiC, Y_2SiO_5 , $Y_2Si_2O_7$, and carbon.

during the plasma wind tunnel testing, the generation of CO gas and the significant pressure increase can result in the formation of blisters (see Fig. 4) near the $Y_2SiO_5/Y_2Si_2O_7$ -SiC interface. Certainly, the critical temperature for expected coating failure depends on the ambient pressure and exposition time, but also on the existence of dispersed carbon inclusions within the underlying CVD-SiC bonding layer.

VI. Conclusions

Plasma wind tunnel tests between 1623 and 1923 K have shown that a two-layer coating system of LPPS yttrium silicates deposited on a CVD-SiC bond coating provides good oxidation protection and erosion resistance for C/C-SiC composites. The relative mass loss was determined to be less than 0.6% and no apparent degradation of the surface material was observed up to 1923 K. At higher temperatures, a formation of local hot spots was visually detected at the sample's surface followed by coating spallation. Overheating effects like these may indicate catalytical interaction between the sample's surface and the plasma flow. Additionally, in view of numerous possible coating failure mech-

anisms a deficiency of mechanical or chemical compatibility between the coating materials and the substrate has to be discussed.

Because of the difference in the thermal expansion coefficients of $Y_2Si_2O_7$ and the two modifications of Y_2SiO_5 , the resulting mechanical strain may also be responsible for microscopic surface cracks and failure during high-temperature application.

Thermodynamic calculations indicate good chemical compatibility between both layer materials, yttrium silicate and SiC. However, increasing partial pressures of oxygen interface reactions at high temperatures are expected from thermodynamic calculations and verified experimentally. As evidenced by calculated isothermal potential phase diagrams, the partial pressure of a formed gaseous phase, mainly consisting of CO and SiO, is of great influence on the interface stability. The formation of gas bubbles and blisters within the silicate layer is obviously resulting from the significantly increasing equilibrium vapor pressure of the system. For atmospheric pressure, a critical surface temperature of 1903 K was predicted by calculations.

Acknowledgments

The authors thank H. Kummer for support in thermal analyses. Special thanks are due to the members of the Institute of Space Systems, University of Stuttgart, for performing plasma wind tunnel tests.

References

- J. R. Strife and J. E. Sheehan, "Ceramic Coatings for Carbon-Carbon Composites," *Am. Ceram. Soc. Bull.*, **67** [2] 369-74 (1988).
- E. Fitzer and L. M. Manocha, *Carbon Reinforcements and Carbon/Carbon Composites*. Springer, Berlin, 1998.
- M. E. Westwood, J. D. Webster, R. J. Day, F. H. Hayes, and R. Taylor, "Review: Oxidation Protection for Carbon Fibre Composites," *J. Mater. Sci.*, **31**, 1389-97 (1996).
- N. S. Jacobson, "Corrosion of Silicon-Based Ceramics in Combustion Environments," *J. Am. Ceram. Soc.*, **76** [1] 3-28 (1993).
- Y. Ogura, M. Kondo, and T. Morimoto, " Y_2SiO_5 as Oxidation Resistant Coating for C/C Composites," pp. 767-74, *Proceedings of the 10th International Conference on Composite Materials (ICCM-10)*, IV, Whistler, BC, Canada, 1995.
- J. D. Webster, M. E. Westwood, F. H. Hayes, R. Taylor, A. Duran, M. Aparicio, K. Rebstock, and W. D. Vogel, "Oxidation Protection Coatings for C/SiC Based on Y_2SiO_5 ," *Key Eng. Mat.*, **132-136**, 1641-4 (1997).
- Y. Ogura, M. Kondo, T. Morimoto, A. Notomi, and T. Sekigawa, "Oxidation Behavior of Y_2SiO_5/SiC Coatings in Low Pressures of Oxygen," *J. Jpn. Inst. Metals*, **65** [1] 12-3 (2001).
- M. Kato, T. Fukasawa, and Y. Goto, "Reactions in Y_2SiO_5 -SiC and $Y_3Al_5O_{12}$ -SiC in Yttrium-Silicate/Silicon Carbide Layered Composites," *J. Ceram. Soc. Jpn.*, **108** [9] 861-4 (2000).
- J. D. Webster, M. E. Westwood, F. H. Hayes, R. J. Day, R. Taylor, A. Duran, M. Aparicio, K. Rebstock, and W. D. Vogel, "Oxidation Protection Coatings for C/SiC Based on Yttrium Silicate," *J. Eur. Ceram. Soc.*, **18**, 2345-50 (1998).
- T. Laux, T. Ullmann, M. Auweter-Kurtz, H. Hald, and A. Kurz, "Investigations of Thermal Protection Materials Along an X-38 Re-entry Trajectory by Plasma Wind Tunnel Simulations," *Proceedings of the 2nd International Symposium, Atmospheric Reentry Vehicles and Systems*, 26-29 March 2001, Arcachon, France, on CD (2001).
- J. Fabig and W. Krenkel, "Tailoring of Microstructure in C/C-SiC Composites," pp. 759-65, *Proceedings of the 10th International Conference on Composite Materials (ICCM-10)*, Vol. IV, Whistler, BC, Canada, 1995.
- N. Saunders and A. P. Miodownik, "CALPHAD (Calculation of Phase Diagrams): A Comprehensive Guide," in *Materials Series*, Vol. 1, Edited by R. W. Cahn, Pergamon, Oxford, 1998.
- B. Sundman, B. Jansson, and J.-O. Andersson, "The Thermo-Calc Databank System," *Calphad*, **9**, 153-90 (1985).
- Scientific Group Thermodata Europe, Grenoble Campus, Saint Martin D'Heres, France, <http://www.sgte.org>.
- J. Gröbner, "Konstitutionsberechnungen im System Y-Al-Si-C-O (Phase Diagram Calculations in the System Y-Al-Si-C-O)," Ph.D. Thesis, University of Stuttgart, 1994.
- V. Swamy, H. J. Seifert, and F. Aldinger, "Thermodynamic Properties of Y_2O_3 Phases and the Yttrium-Oxygen Phase Diagram," *J. Alloys Comp.*, **269**, 201-7 (1998).
- B. Hallstedt, "Thermodynamic Assessment of the Silicon-Oxygen System," *Calphad*, **1**, 53-61 (1992).
- U. Kolitsch, "Hochtemperaturkalorimetrie und Phasenanalytik in SE_2O_3 - Al_2O_3 - SiO_2 Systemen (High Temperature Calorimetry and Phase Analysis in RE_2O_3 - Al_2O_3 - SiO_2 Systems)," Ph.D. Thesis, University of Stuttgart, 1995.
- J.-J. Liang, A. Navrotsky, T. Ludwig, H. J. Seifert, and F. Aldinger, "Enthalpy of Formation of Rare-Earth Silicates Y_2SiO_5 and Yb_2SiO_5 and N-containing Silicate $Y_{10}(SiO_4)_6N_2$," *J. Mater. Res.*, **14** [4] 1181-5 (1999).

²⁰O. Fabrichnaya, H. J. Seifert, R. Weiland, T. Ludwig, F. Aldinger, and A. Navrotsky, "Phase Equilibria and Thermodynamics in the Y_2O_3 - Al_2O_3 - SiO_2 System," *Z. Metallkd.*, **92**, 1083–97 (2001).

²¹J. Felsche, "Crystal Data on the Polymorphic Disilicate $Y_2Si_2O_7$," *Naturwissenschaften*, **57**, 127–8 (1970).

²²K. Liddell and D. P. Thompson, "X-ray Diffraction Data for Yttrium Silicates," *Br. Ceram. Trans. J.*, **85**, 17–22 (1986).

²³J. W. Nowok, J. P. Kay, and R. J. Kulas, "Thermal Expansion and High-Temperature Phase Transformation of the Yttrium Silicate Y_2SiO_5 ," *J. Mater. Res.*, **16** [8] 2251–5 (2001).

²⁴R. Henne, "Direct Current Plasma Torches for Thermal Spraying—Present Status and New Developments," *Weld. Cutting*, **2**, E31–5 (1993).

²⁵T. Ullmann, M. Schmücker, H. Hald, R. Henne, and H. Schneider, "Oxidation Protection of C/SiC Composites Based on Plasma-Sprayed Y-Silicates;" *Proceedings of the 8th International Symposium on Materials in Space and Environment and 5th International Conference on Protection Materials and Structures from LEO Space Environment*, 5–9 June 2000, Arcachon, France, on CD, 2000.

²⁶M. Auweter-Kurtz, H. Habiger, H. Kurtz, S. Laure, W. Röck, and N. Tubanos, "Die Plasmawinkanäle PWK-IRS-Werkzeuge zur Untersuchung von Hitzeschutzmaterialien für Rückkehrfahrzeuge," *Z. Flugwiss. Weltraumforsch.*, **17**, 1–15 (1993).

²⁷T. Ullmann, H. Hald, O. Vollrath, H. H. Grotheer, O. Haidn, and M. Auweter-Kurtz, "Behaviour of C/C–SiC Material in Reentry and H_2/O_2 Combustion Environment;" pp. 291–301, *Proceedings of the 3rd European Workshop on Thermal Protection Systems*, 25–27 March 1998, ESA-WPP-141, 1998.

²⁸M. Aparicio and A. Duran, "Yttrium Silicate Coatings for Oxidation Protection of Carbon–Silicon Carbide Composites," *J. Am. Ceram. Soc.*, **83** [6] 1351–5 (2000).

²⁹M. Aparicio, R. Moreno, and A. Duran, "Colloidal Stability and Sintering of Yttria–Silica and Yttria–Silica–Alumina Aqueous Suspensions," *J. Eur. Ceram. Soc.*, **19**, 1717–24 (1999).

³⁰S. Wagner, H. J. Seifert, and F. Aldinger, "High Temperature Reactions of C/C–SiC Composites with Ceramic Coatings;" pp. 71–8 in *Proceedings of the International Conference on Advances in Materials and Materials Processing, ICAMMP-2002*, 1–3 February 2002, Kharagpur, India. Edited by N. Chakraborti, and U. K. Chatterjee. Tata McGraw-Hill, New Delhi, 2002.

³¹W. L. Vaughn and H. G. Maahs, "Active-to-Passive Transition in the Oxidation of Silicon Carbide and Silicon Nitride in Air," *J. Am. Ceram. Soc.*, **73** [6] 1540–3 (1990).

³²T. Goto, T. Narushima, Y. Iguchi, and T. Hirai, "Active to Passive Transition in the High-Temperature Oxidation of CVD SiC and Si_3N_4 ;" pp. 165–76 in *Corrosion of Advanced Ceramics*, Edited by K. G. Nickel. Kluwer Academic Publishers, The Netherlands, 1994.

³³T. Goto, H. Homma, and T. Hirai, "Effect of Oxygen Partial Pressure on the High-Temperature Oxidation of CVD SiC," *Corrosion Sci.*, **44**, 359–70 (2002).

³⁴A. H. Heuer and V. L. K. Lou, "Volatility Diagrams for Silica, Silicon Nitride, and Silicon Carbide and Their Application to High-Temperature Decomposition and Oxidation," *J. Am. Ceram. Soc.*, **73** [10] 2789–803 (1990).

³⁵K. Brennfleck, G. Porsch, H. Reich, and H. J. Scheiffarth, "CVD of SiC on an Industrial Scale," *Proc. Int. Conf. CVD, CVD-XI*, 395–403 (1990). □